The Helix-Hinge-Helix Structural Motif in Human Apolipoprotein A-I Determined by NMR Spectroscopy[†,‡]

Guangshun Wang,[§] James T. Sparrow,[||] and Robert J. Cushley*[,§]

Institute of Molecular Biology and Biochemistry, Simon Fraser University, Burnaby, British Columbia, Canada V5A 1S6, and Department of Medicine, Baylor College of Medicine, One Baylor Plaza, Houston, Texas 77030

Received May 16, 1997; Revised Manuscript Received August 15, 1997[⊗]

ABSTRACT: The conformation of a synthetic peptide of 46 residues from apoA-I was investigated by fluorescence, CD, and 2D NMR spectroscopies in lipid-mimetic environments. ApoA-I(142−187) is mainly unstructured in water but helical in SDS or dodecylphosphocholine (DPC), although the peptide only associates with DPC at approximately the critical micellar concentration. Solution structures of apoA-I(142−187) were determined by distance geometry calculations based on 450 (in DPC-d_{38}) or 397 (in SDS-d_{25}) NOE-derived distance restraints, respectively. Backbone RMSDs for superimposing the two helical regions 146−162 and 168−182 are 0.98 ± 0.22 (2.38 ± 0.20) and 1.99 ± 0.42 (2.02 ± 0.21) Å in DPC (SDS), respectively. No interhelical NOE was found, suggesting that helix−helix interactions between the two helical domains in apoA-I(142−187) are unlikely. Similar average, curved helix-hinge-helix structures were found in both SDS and DPC micelles with the hydrophobic residues occupying the concave face, indicating that hydrophobic interactions dominate. Intermolecular NOESY experiments, performed in the presence of 50% protonated SDS, confirm that the two amphipathic helices and Y166 in the hinge all interact with the micelle. The involvement of Y166 in lipid binding is supported by fluorescence spectroscopy as well. On the basis of all the data above, we propose a model for the peptide−lipid complexes wherein the curved amphipathic helix-hinge-helix structural motif straddles the micelle. The peptide-aided signal assignment achieved for apoA-I(122−187) (66mer) and apoA-I suggests that such a structural motif is retained in the longer peptide and most likely in the intact protein.

Human apoA-I[1] is the principal protein component (∼70%) of HDL. Interest in the study of apoA-I is high due to its protective effect against atherosclerosis (Breslow, 1996). Such an effect of apoA-I is not well understood but may be attributed to its role in reverse cholesterol transport (Glomset, 1968) as a probable ligand for the HDL receptor (Acton et al., 1996), in LCAT activation (Fielding et al., 1972) and in cholesterol efflux (Castro & Fielding, 1988; Zhao et al., 1996).

ApoA-I contains a single polypeptide chain of 243 amino acid residues (Brewer et al., 1978) with regular 11 or 22 residue repeating units in the sequence (McLachlan, 1977). These multiple repeats were proposed to form amphipathic helices with distinct hydrophilic and hydrophobic faces (Segrest et al., 1974). The major secondary structure of apoA-I was predicted to contain 6−9 helical segments linked by β-turns (Jonas et al., 1989; Brasseur et al., 1990; Segrest et al., 1994). Sparrow and Gotto (1982) showed that apoA-I(197−243) bound to DMPC but did not activate LCAT. Such an observation is consistent with deletion of a similar segment from apoA-I either by proteolysis (Ji & Jonas, 1995) or by expression of gene knock-out mutants (Schmidt et al., 1995; Holvoet et al., 1996). Wang et al. (1996a) have recently attributed the strong lipid binding of the C-terminus of apoA-I or apoE to numerous aromatic residues and hydrophobic residue pairs in the sequence, which play a crucial role in anchoring apolipoproteins to lipid (Sparrow & Gotto, 1982; Rozek et al., 1995; Buchko et al., 1996a,b; Wang et al., 1996b). On the other hand, truncation of the N-terminal residues 1−43 from apoA-I was believed to have little effect on LCAT activation (Rogers et al., 1997). On the basis of the finding that the consensus sequence with a Glu residue at the 13th position best activates LCAT, Anantharamaiah et al. (1990) proposed that the major LCAT-activating domain is within residues 66−120. While monoclonal antibody studies by Banka et al. (1991) also suggest a similar region, Meng et al. (1993) and Uboldi et al. (1996) found that, within the region 96−174 of apoA-I, several putative helices are implicated in LCAT activation. More recent site-directed mutagenesis studies point to the

[†] Research was supported by the Natural Sciences and Engineering Research Council of Canada.

[‡] Brookhaven Protein Data Bank identification numbers: 1GW3 (coordinates) and R1GW3MR (restraints) for apoA-I(142−187) in DPC; 1GW4 (coordinates) and R1GW4MR (restraints) for apoA-I(142−187) in SDS.

* Corresponding author. Email: cushley@sfu.ca.

[§] Simon Fraser University.

[||] Baylor College of Medicine.

[⊗] Abstract published in *Advance ACS Abstracts,* October 1, 1997.

[1] Abbreviations: ApoA-I, apolipoprotein A-I; SDS, sodium dodecyl sulfate; DPC, dodecylphosphocholine; HDL, high density lipoproteins; LCAT, lecithin:cholesterol acyltransferase; CETP, cholesteryl ester transfer protein; DMPC, dimyristoylphosphatidylcholine; CMC, critical micellar concentration; TFA, trifluoroacetic acid; DMF, dimethylformamide; t-Boc, *tert*-butoxylcarbonyl; DIEA, diisopropylethylamine; HOBT, 1-hydroxybenzotriazole; HBTU, 2-(1H-benzotriazol-1-yl)-1,1,3,3-tetramethyluronium hexafluorophosphate; TMSBr, trimethylsilyl bromide; DCM, dichloromethane; GdnHCl, guanidine hydrochloride; DSS, sodium 2,2-dimethyl-2-silapentane-5-sulfonate; CD, circular dichroism; NMR, nuclear magnetic resonance; NOESY, two-dimensional nuclear Overhauser enhancement spectroscopy; τ_m, mixing time; TOCSY, total correlation spectroscopy; DQF-COSY, double-quantum filtered correlation spectroscopy; RMSD, root mean square deviation; CSI, chemical shift index; HPLC, high performance liquid chromatography.

S0006-2960(97)01151-3 CCC: $14.00

Table 1: Properties of the Two Model Lipids Used to Model HDL

	SDS[a]	DPC[b]	HDL_3[c]
head group net charge	−1	0	0
CMC (mM)	8	1.2	
lipid molecules/particle	62	56	51[d]
particle MW	19 500	21 600	∼175 000
diameter (Å)	∼50	47−55	40−70
axial ratio (*b*/*a*)	2	6	∼1

[a] Mysels and Pricen (1959), Helenius and Simons (1975), and Reynolds (1982). [b] Lauterwein et al. (1979). [c] Scanu et al. (1982). [d] Number of phospholipid molecules.

importance of residues 120−187 in LCAT activation (Sorci-Thomas et al., 1993, 1997; Minnich et al., 1992; Holvoet et al., 1995). In addition, the region 122−187 was shown to play a role in cholesterol efflux (Fielding et al., 1994; Sviridov et al., 1996). Synthetic peptides apoA-I(121−164) (Fukushima et al., 1980) and apoA-I(145−185) (Sparrow & Gotto, 1980) were both shown to bind DMPC, to adopt helical conformations and to activate LCAT to 30 and 25% of apoA-I, respectively. These "44mers" are believed to be the paradigm of apoA-I (Nakagawa et al., 1985).

The sequence of apoA-I(120−187), composed of 22mer repeats 4, 5, and 6, is unique in that it contains few aromatic residues, no hydrophobic residue pairs, but is rich in arginines. Because of the potential biological significance of this region of apoA-I, we report the chemical synthesis and conformational studies of two peptides, apoA-I(142−187) and apoA-I(122−187), using SDS or DPC as model lipids. HDL is a quasi-spherical particle consisting of a core of cholesteryl esters surrounded by a monolayer of phospholipid. Embeded in the monolayer are the apolipoproteins apoA-I, A-II, C-I, C-II, C-III, and E. Particle sizes range from 40 to 70 Å in diameter for HDL_3. It is known that pre-βHDL (the smallest HDL) and HDL_3 are better substrates for LCAT than HDL_2. SDS and dodecylphosphocholine (DPC) are commonly used to model membranes (McDonnell & Oppella, 1993; Henry & Sykes, 1994). Both form micelles ∼50 Å in diameter, i.e., equal to the smallest HDL_3, Table 1. DPC has the same head group as phospholipids; however, we chose SDS because it gives the best resolved NMR spectra which are needed for a protein the size of apoA-I. Similar structures were obtained for the LCAT activating *de novo* peptide LAP-20 in the presence of both SDS and DPC, and we proposed that both detergents may be used interchangeably to model the lipoprotein environment (Buchko et al. 1996a). In fact, the structure of apoA-I(166−185) in SDS and DPC is even more striking since, not only do the helical backbones superimpose, but most of the side chains adopt similar orientations, on average (Wang et al., 1996b).

In the present study, the solution structure of apoA-I(142−187) in deuterated SDS or DPC micelles was determined by distance geometry based on NOE-derived distances. The interaction of apoA-I(142−187) with SDS or DPC was investigated by CD, fluorescence spectroscopy, and NMR. In addition, we have obtained high-resolution ^{1}H-NMR spectra of intact apoA-I (243 amino acids) in the presence of SDS. Spectral identity between NOESY spectra of apoA-I fragments and the intact protein has led to the assignment of resonances in apoA-I.

MATERIALS AND METHODS

SDS was purchased from BDH (Poole, U.K.). Deuterated SDS (SDS-d_{25}, 98% D) and DPC (DPC-d_{38}) (98.9% D) were purchased from Cambridge Isotope Laboratories (MA) and CDN Isotopes (PQ, Canada), respectively. Deuterium oxide (99.9% D) was a product of Isotec Inc. (OH). ApoA-I(166−185) was purchased from Dr. Ian Clark Lewis, University of British Columbia. Boc-protected amino acids were purchased from Peptides International (Louisville, KY), TFA from Halocarbon Products (Riveredge, NJ), DIEA and HOBT in DMF from Applied Biosystems, Inc. (Foster City, CA), and HBTU from Anaspec (San Jose, CA). TMSBr, thioanisole and ethanedithiol were purchased from Aldrich (Milwaukee, WI) and all solvents were from Burdick and Jackson (Muskegon, MI).

Chemical Synthesis of ApoA-I(142−187) and ApoA-I(122−187). ApoA-I(142−187), SPLGEEMRDRARAHVDALRTHLAPYSDELRQRLAARLEALKENGGA, and apoA-I(122−187), LRAELQEGARQKLHELQEKLSPLGEEMRDRARAHVDALRTHLAPYS-DELRQRLAARLEALKENGGA, were synthesized by the solid phase method as developed by Merrifield (Barany & Merrifield, 1980) using phenylacetamidomethyl polystyrene (Sparrow, 1976) and fast Boc chemistry utilizing HBTU/HOBT coupling (Reid & Simpson, 1992; Sparrow & Monera, 1996) on an ABI 430A synthesizer as implemented in our laboratories. The carboxyl terminal amino acid protected with the *N-tert*-butyloxycarbonyl group was esterified to bromomethylphenylacetic acid and coupled to aminomethyl polystryene resin. Using the fast Boc/HBTU/HOBT synthesis protocol (Reid & Simpson, 1992; Sparrow & Monera, 1996), the total program time per residue was 45 min. TFA (100%) was used to deprotect the amino group in 6 min; the resulting salt was neutralized by the excess DIEA used to activate the *N-tert*-butyloxycarbonyl amino acid with HBTU/HOBT in DMF, thus combining the coupling and neutralization steps. The *N-tert*-butyloxycarbonyl amino acid was activated in the cartridge with 0.48 M HBTU/0.5 M HOBT in DMF and 6 equiv of DIEA; the activated amino acid was transferred directly to the reactor vessel. The coupling reaction was allowed to proceed for 15 min and the resin washed extensively with DMF and DCM. These steps were then repeated until the sequence of interest had been synthesized. Arg, Asn, His and Thr were doubly coupled. After the addition of Boc(Xan)Gln, the amino acid was deprotected with 60% TFA/DCM instead of 100% TFA in order to prevent premature chain termination by cyclization of the Gln to pyroglutamyl (J. T. Sparrow, unpublished results). The following side-chain protection was used: 2,6-dichlorobenzyl for the hydroxyl of tyrosine, benzyl for the hydroxyl of serine and threonine; benzyl ester for the β- and γ-carboxyl of aspartic and glutamic acid; 2-chlorobenzyloxycarbonyl for the ϵ-amino of lysine, benzyloxymethyl for the imidazole of histidine, trimethylbenzenesulfonyl for the guanidino of arginine, and xanthanyl for the amido of glutamine and asparagine.

TMSBr/TFA Peptidyl-resin Cleavage and Deprotection. Following the procedure of Sparrow and Monera (1996), 1 g of peptidyl-resin was placed in a dry 100 mL round-bottom flask protected with a $CaSO_4$ drying tube. The resin was stirred as 12 mL of thioanisole and 1.0 mL of ethanedithiol were added followed by 50 mL of TFA. The cleavage

mixture was cooled to −10 °C with stirring; 7.0 mL of TMSBr was added, and the stirring at −10 °C continued for 10 min. The flask was then transferred to a stirrer at room temperature and connected to a N_2 source. Stirring was continued for 2.5 h at room temperature under N_2 and the flask protected from light with Al foil. The reaction mixture was filtered into a 250 mL round-bottom flask, and the flask, filter, and resin were washed with 2 × 10 mL of TFA. The excess HBr was removed on the rotary evaporator under house vacuum to prevent bumping and then the evaporator transferred to a vacuum pump to remove the TFA at 35 °C. The peptide was precipitated with ether, filtered, and washed with ether. The dry powder was dissolved in 1 M Tris/6 M GdnHCl. After adjusting the pH to 3.0, the peptide was desalted on a Bio-Gel P-2 column equilibrated with 5% acetic acid. The peptide fractions were identified by absorbance at 275 nm, pooled, and lyophilized.

Peptide Purification and Characterization. The peptides were purified by reversed-phase HPLC (Hancock & Sparrow, 1981 & 1984) as follows: the peptide (50−100 mg in 5 mL of water) was diluted with 20 mL of 1% TFA and 6 M GdnHCl and the solution pumped onto a 2.5 × 25 cm Vydac C4 column equilibrated in 0.1% TFA. The peptide was eluted with a linear gradient between 0.1% TFA and 0.1% TFA and 70% 2-propanol at a flow rate of 20 mL/min. The peptide was detected by absorbance at 254 and 280 nm; the peptide-containing fractions were pooled and lyophilized. The peptide was dissolved in water and the following criteria were applied to evaluate the purity of the synthetic product: (1) analytical HPLC on a 5 μm Vydac C18 column (0.46 × 25 cm) using a linear gradient of 0.1% TFA and 2-propanol at a flow rate of 1 mL/min; (2) amino acid analysis for correct composition; (3) Automatic amino acid sequencing; and (4) electrospray mass spectrometry. The expected mass for apoA-I(142−187) is 5141.8, found 5142.3; and that expected for apoA-I(122−187) is 7513.5, found 7514.6.

Circular Dichroism. CD spectra were recorded on a Jasco J710 spectropolarimeter at 37 °C as described previously (Wang et al., 1996a). The peptide concentration was measured using UV absorbance of Y166 at 280 nm (ϵ = 1280 $cm^{-1}M^{-1}$) (Gill & von Hippel, 1989). The helix content was estimated using convex constraint analysis (Perczel et al., 1991).

Fluorescence Spectroscopy. Fluorescence measurements were performed on an SLM4800C spectrofluorometer at 20 °C. Samples of apoA-I(142−187) and the standard tyrosine (Narayanaswami et al., 1993) were excited at 277 nm, and emission was recorded from 270 to 350 nm. The excitation and emission band widths were both 8 nm. The relative quantum yield (Q_x) was calculated (Freifelder, 1976):

$$Q_x = (Q_s I_x A_s)/(I_s A_x)$$

where Q_x and Q_s are the quantum yield of the unknown and standard samples, respectively, I_x and I_s are the integrated intensities of the unknown and standard samples, and A_x and A_s are the optical density of the unknown and standard at 277 nm.

Nuclear Magnetic Resonance. The NMR samples containing 5 mM apoA-I(142−187) or apoA-I(122−187) and 300 mM SDS-d_{25} or DPC-d_{38} (1:60, mol/mol) were prepared in 0.5−0.6 mL of 90% H_2O and 10% D_2O solution. ApoA-I, obtained from the Swiss Red Cross, was dissolved in 0.5 mL of H_2O/D_2O (9:1) at an apoA-I concentration of 3 mM and the protein/SDS molar ratio of 1:140 (Reynolds, 1982). The pH of the sample was measured in the 5 mm NMR tube with a glass electrode (meter reading) and adjusted using small fractions of NaOH or HCl solution.

NOESY (Jeener et al., 1979), TOCSY (Braunschweiler et al., 1983; Bax & Davis, 1985), and DQF-COSY (Rance et al., 1983) were acquired at a ^1H resonance frequency of 600.13 MHz on a Bruker AMX 600 spectrometer in the phase-sensitive mode using time-proportional phase incrementation (TPPI) (Marion & Wüthrich, 1983; Redfield & Kunz, 1975). In t_2, 2K data points were collected at a spectral width of 6250 Hz. There were 560 increments in t_1 with 64 scans each. NOESY spectra were collected at a mixing time of 300 ms for spectral assignments and 50−100 ms for structural calculations. TOCSY experiments were collected at a mixing time of 100 ms with a 2.5 ms trim pulse before the MLEV-17 spin-locking sequence. During data acquisition, the water signal was suppressed by the WATERGATE technique (Piotto et al., 1992) using a 3-9-19 pulse sequence (Sklenár et al., 1993) for TOCSY and NOESY. In the DQF-COSY experiments, the water signal was suppressed by presaturation during the relaxation delay. The water resonance was further suppressed during data processing using the convolution difference low-pass filter technique (Marion et al., 1989). NMR spectra were apodized by a shifted sine-bell window function: 90° in F_2 and 0° in F_1. After zero-filling to 2K × 2K, the spectra were Fourier-transformed on an Aspect X32 workstation using UXNMR software (Bruker) or the FELIX95 (Biosym Technologies, Inc.) program on an Indigo2 Computer (Silicon Graphics, Inc.). Baselines were corrected using a fifth-order polynomial function in both dimensions. All chemical shifts were referenced to the methyl signals of sodium 4,4-dimethyl-4-silapentane-1-sulfonate (DSS) as an internal standard.

Structure Calculation. Distance restraints for structural calculations were generated from the NOESY spectra (80 ms in DPC and 100 ms in SDS) by classifying NOE cross-peaks into strong (1.8−2.8 Å), medium (1.8−3.8 Å), and weak (1.8−5.0 Å) based on the volumes of cross-peaks (Gronenborn & Clore, 1995), calibrated using known distances in the α-helix structure (Wüthrich, 1986; Cavanagh et al., 1996). Pseudoatom corrections were made for unresolved methylene, methyl, and Tyr aromatic protons by adding 1.0, 1.5, and 2.0 Å, respectively, to the upper bounds of pertinent restraints (Wüthrich et al., 1983). An additional 0.5 Å was added to the distance upper bounds involving methyl group protons (Clore et al., 1987).

Using NOE distance restraints, along with the geometric and chiral restraints from an extended covalent structure of the peptide with planar, *trans* peptide bonds, structures were calculated by metric matrix distance geometry techniques (Havel, 1991) on an Indigo2 workstation with the program DGII of InsightII (Biosym Technologies, Inc.). In a first step, these restraints were triangle and tetrangle smoothed sequentially. Following smoothing, restraints were then embedded in four dimensions and converted to three dimensional coordinates after optimization. The initial energy for annealing was previewed and 1700 kcal/mol was found to be proper. Simulated annealing was performed by "cooking" to 200 K and "cooling" at 2.1 × 10^{-13} s per step to 0 K. The structures were energy minimized using a conjugate gradient algorithm. After iterative refinements,

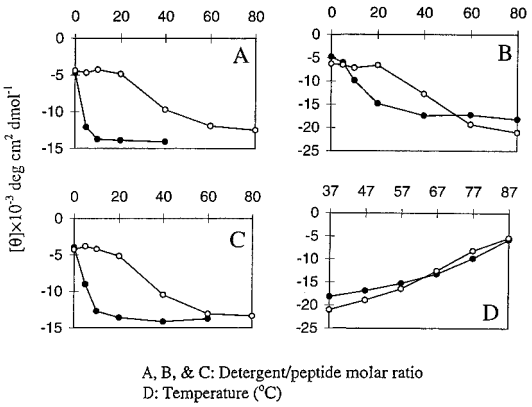

FIGURE 1: Variation of the molar ellipticity at 222 nm of the CD spectra of 0.1 mM apoA-I(166−185) (A), 0.035 mM apoA-I(142−187) (B), and apoA-I(122−187) (C) with the addition of SDS (solid circles) or DPC (open circles), at pH 6−7, 37 °C. (D) Change of the molar ellipticity at 222 nm of the CD spectra of apoA-I(142-187) complexed with SDS (solid circles) or DPC (open circles) as a function of temperature. The samples are the final stages in panel B, that is, at the detergent/peptide molar ratio of 80:1, pH 6−7.

distance violations greater than 0.1 Å were listed and examined. Upper limits for those that were consistently greater than 0.2 Å were relaxed to an upper class. The structures showed no distance violation greater than 0.3 Å determined in SDS and no distance violation greater than 0.5 Å in DPC. On average, the distance violation per residue from 0.1 to 0.5 Å is 1.1 in SDS and 1.0 in DPC whereas the distance violation from 0.05−0.5 Å per residue is 4.8 in SDS and 5.0 in DPC.

RESULTS

Circular Dichroism. ApoA-I(142−187) and apoA-I(122−187) lack ordered structures in the absence of lipid as indicated by the negative CD band at 203 nm (Woody, 1995). Convex constraint analysis (Perczel et al., 1991) of the CD data gave 15% helix and 47−50% random coil for both fragments. The solution of these peptides became turbid at a peptide/SDS molar ratio of approximately 1:5 at pH < 5. The turbidity disappeared upon increase of pH or further addition of SDS. A similar phenomenon was observed for apoC-I peptides (Rozek et al., 1995). O'Neil and Sykes (1989) have attributed this effect to salt formation between the negatively charged SDS and the positively charged N-terminus of the peptide. Above a peptide/SDS ratio of 1:40, the CD curves for both peptides were characterized by double minima at 207−209 and ∼222 nm and a strong positive band at ∼195 nm, indicating α-helix (Holzwarth & Doty, 1965).

Figure 1 shows the variation of the 222 nm band of apoA-I(166−185) (A), apoA-I(142−187) (B), and apoA-I(122−187) (C) with the addition of DPC or SDS at pH 6−7. While the molar ellipticity at the 222 nm band for all three peptides changed with the addition of SDS below the CMC, no apparent change occurred upon titration with DPC until the DPC concentration approached the CMC (approx. 1.2 mM, Lauterwein et al., 1979). From convex constraint analysis, the estimated helix contents of apoA-I(142−187) and apoA-I(122−187) are 62% (peptide/SDS, 1:80) and 56% (peptide/SDS, 1:60), respectively. ApoA-I(142−187) contains 69% helix in DPC and 74% in an SDS/DPC (1:1) mixture (peptide/lipid, 1:80). Vanloo et al. (1995) reported 59% helix for apoA-I(145−183) in DMPC and 56% in trifluoroethanol.

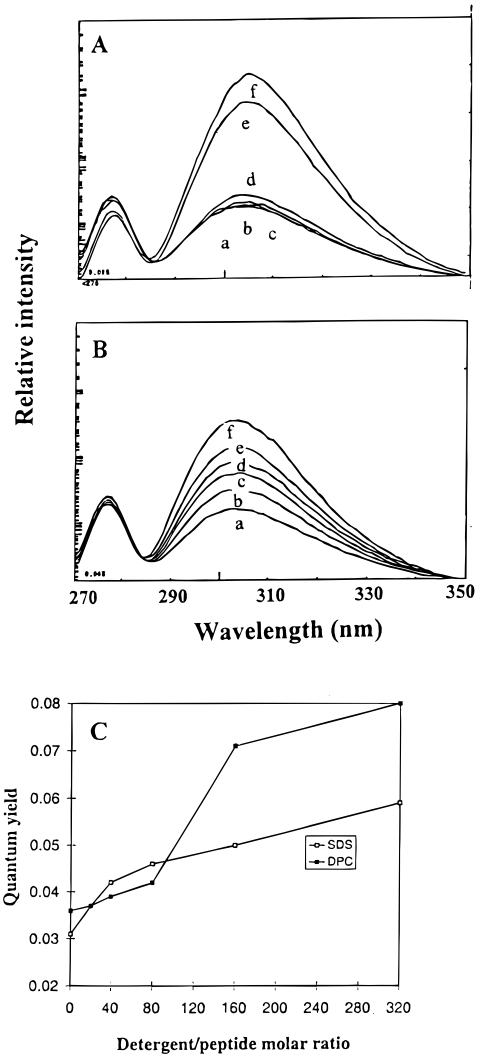

FIGURE 2: Increase of fluorescence intensity with the addition of DPC (A) or SDS (B). Detergent/peptide molar ratios are $a = 0$, $b = 20$, $c = 40$, $d = 80$, $e = 160$, and $f = 320$ at pH 6−7, 20 °C. (C) Plot of the quantum yield of apoA-I(142−187) against the detergent/peptide molar ratio. Relative quantum yields were calculated as detailed in Materials and Methods. The samples were excited at 277 nm and emissions recorded from 270 to 350 nm. The excitation and emission band widths were both 8 nm.

To compare the stability of the helical structure of apoA-I(142−187) in the bound state, the peptide−lipid complexes were heated from 37 to 87 °C (Figure 1D). The peptide/lipid ratio was 1:80. The decrease in the value of the molar ellipticity at 222 nm indicates less helical conformation with increase of temperature. Linear regression of molar ellipticity values at 222 nm *versus* temperature yielded the slopes of 327 and 245 deg cm^2 dmol^{-1} °C^{-1} in DPC and SDS, respectively, indicating that the stability of the peptide−SDS complexes is greater than the peptide−DPC complexes.

Fluorometric Study. ApoA-I(142−187) contains a single tyrosine, Y166, located in the putative β-turn region. Y166 fluoresces at 305 nm, and the fluorescence intensity increases upon titration with either DPC or SDS, Figure 2, panels A and B, respectively, indicating complex formation. The relative quantum yield of Y166 in apoA-I(142−187) was calculated at various levels of SDS or DPC, and the results are plotted in Figure 2C. Upon addition of SDS to the peptide, the quantum yield of Y166 increased monotonically from 0.031 in water to 0.059 in SDS/peptide (molar ratio 320:1), whereas the addition of DPC to apoA-I(142−187)

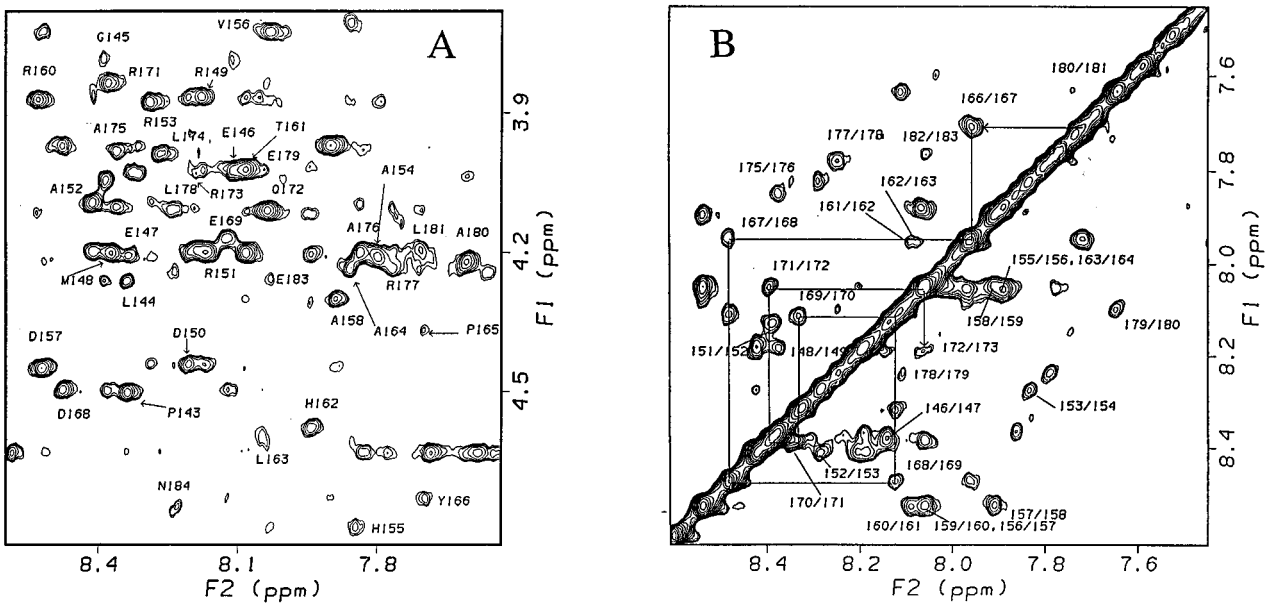

FIGURE 3: The fingerprint (A) and amide proton (B) regions of the NOESY spectra of apoA-I(142−187) (5 mM) in aqueous solution (H_2O/D_2O, 9:1) of DPC-d_{38} (τ_m = 80 ms) at 37 °C (peptide/lipid molar ratio = 1:60) at pH 4.9. $H^{\alpha}-H^{N}$ peaks for each residue (A) and amide−amide cross peaks (B) are labeled. For clarity, only the seqential assignments for residues 166−172 were constructed in panel B.

gave little change in the fluorescence spectrum or quantum yield when the DPC/peptide ratio was below approximately 80:1 (Figure 2, panels A and C). However, the intensity and quantum yield increased dramatically at the DPC/peptide ratio of 160:1, i.e., a DPC concentration of 1.6 mM. An increase in tyrosine's quantum yield reflects a change in its chemically bonded state, possibly the different H-bonding of the phenolic group to lipid head group versus water. The increase in fluorescence intensity as lipid is added and the increased quantum yield are consistent with apoA-I(142−187) associating with lipid (Narayanaswami et al., 1993). The behavior in the presence of DPC indicates that the peptide only associates after DPC forms micelles.

NMR Assignments of ApoA-I(142−187) Bound to SDS or DPC. Figure 3 presents the fingerprint (A) and amide (B) proton regions of the NOESY spectrum of apoA-I(142−187) in DPC micelles. As fewer TOCSY H^N to side-chain cross-peaks were available, assignments were achieved by combining the sequential (Wüthrich, 1986) and the main-chain directed approach (Englander & Wand, 1987). For example, the side chain of the single valine gave two sets of NOE connectivities. The stronger ones resulted from the H^N of V156 to its H^{α}, H^{β}, and H^{γ}, whereas the medium to weak ones were assigned as the NOE connectivies of V156 to the H^N of D157. From D157, A158 was deduced using the $H_i^{\beta}-H_{i+1}^{N}$ connectivity. Other useful starting spin systems were Y166, D150, H155, H162, and the seven alanines. The assignment of Y166 and the histidines was facilitated by the NOE connectivities of H^{β} to both H^N and the aromatic ring protons. The spin systems were then linked using $H_i^{\alpha}-H_{i+1}^{N}$, $H_i^{\alpha}-H_{i+3}^{\beta}$, and $H_i^{N}-H_{i+1}^{N}$ NOE connectivities as shown in Figure 3B. The H^{α} and side-chain resonances were confirmed by TOCSY spin patterns and the assignment of side chains was corroborated by DQF-COSY.

Spectra of apoA-I(142−187) in SDS micelles were run at 50 °C due to limited resolution in the amide region at 37 °C. The fingerprint region of the NOESY spectrum of the peptide in SDS at pH 4.9 and 50 °C is given in Figure 4. Since H^{α} signals of D150 and D157 resonated near the water

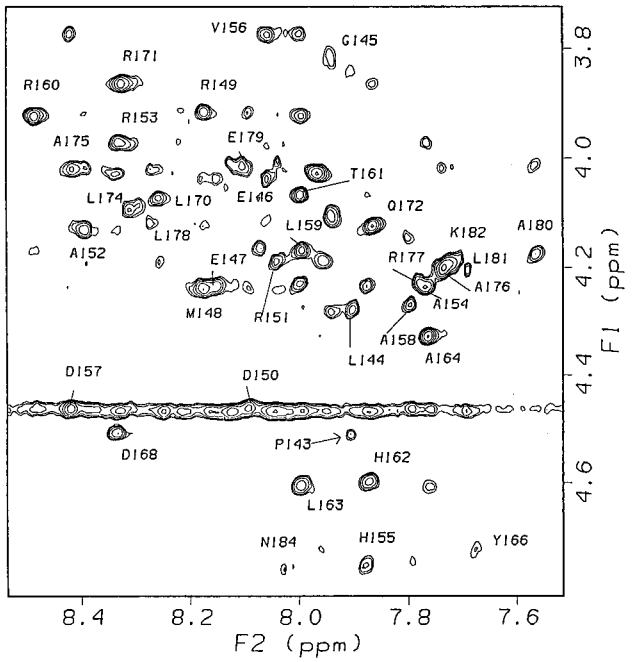

FIGURE 4: The fingerprint region of the NOESY spectrum of apoA-I(142−187) (5 mM) in acqueous solution (H_2O/D_2O, 9:1) of SDS-d_{25} (τ_m = 100 ms) at 50 °C, pH 4.9. The peptide/SDS molar ratio is 1:60. The $H^{\alpha}-H^{N}$ cross peak of each residue is labeled.

signal at 50 °C in SDS, they were confirmed at 37 °C. C-terminal residues G185, G186, and A187 were assigned using the zero-quantum dispersive peaks observed in the NOESY spectrum at 50 ms (Cavanagh et al., 1996). Comparison of the spectra in SDS and DPC confirmed the assignment for G145, E146, D168, and E169, which are weak or missing in SDS. In addition, the side-chain ϵH^N signals of arginines of apoA-I(142−187) resonate between 7.49 and 7.83 ppm in DPC but between 7.08 and 7.26 ppm in SDS. These side-chain signals in SDS do not overlap with amide proton resonances of the peptide, thus confirming their assignments in DPC. Tables of chemical shifts are included in the Supporting Information.

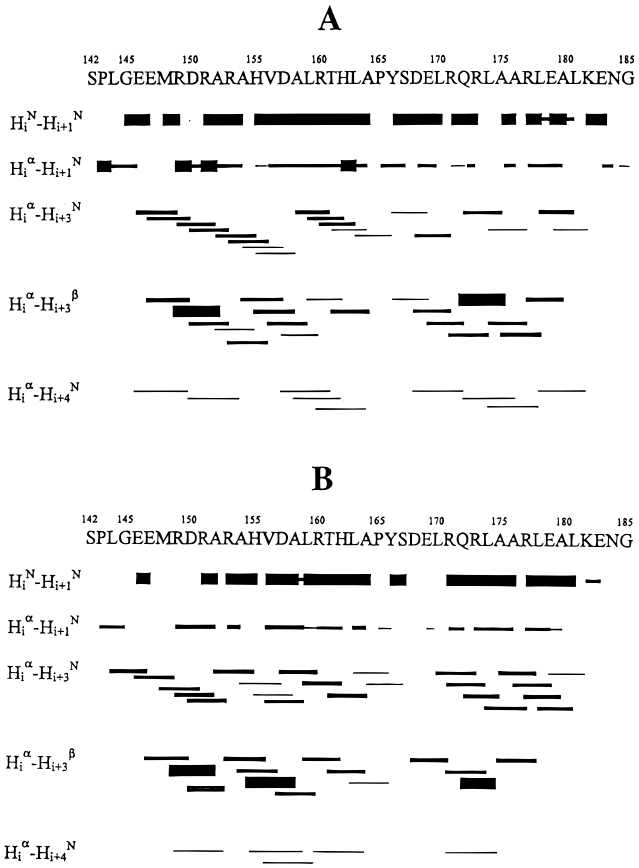

FIGURE 5: Summary of interresidue NOE connectivities of apoA-I(142−187) bound to DPC (A) and SDS (B) micelles. Strong, medium, and weak NOEs are depicted with bars of different heights.

Secondary Structure of ApoA-I(142−187) in SDS or DPC. H^α secondary shifts were calculated by subtracting the chemical shifts in unstructured peptides (Wüthrich, 1986) from the measured chemical shifts and converted to CSIs (Wishart et al., 1992). A grouping of CSI = +1 indicates β-strand and a grouping of CSI = −1 indicates a helical structure. The CSI values are included in the chemical shift tables in the Supporting Information. From the CSI values, apoA-I(142−187) was predicted to contain two helical regions, 145−162 and 168−182, in either SDS or DPC. A comparison of chemical shifts of apoA-I(142−187) in SDS and DPC revealed that, except for S142, R153, A164, R173, and L174, whose H^α chemical shifts differ by 0.12 ppm or less, all chemical shift differences are within ±0.05 ppm, suggesting a similar conformation in the two lipid-mimetic environments.

The interresidue NOEs for apoA-I(142−187) in DPC (A) and SDS (B) micelles are summarized in Figure 5. In both micellar systems, a combination of NOE patterns such as medium to strong $H_i^N-H_{i+1}^N$, weak to medium $H_i^\alpha-H_{i+3}^N$, weak to strong $H_i^\alpha-H_{i+3}^\beta$, $H_i^\alpha-H_{i+1}^N$, and weak $H_i^\alpha-H_{i+4}^N$ indicates helix structures in regions corresponding to residues 146−164 and 168−182. The H^N signals of both A164 and Y166 showed NOE cross-peaks with the H^δ of P165, indicating a predominantly *trans* conformation for the proline in both micelles (Wüthrich et al., 1984). A similar proline conformation has been found in apoE(263−286) associated with SDS micelles (Wang et al., 1996a).

Structures of ApoA-I(142−187) in DPC and SDS. Figure 6 shows the backbone view of the calculated structures of

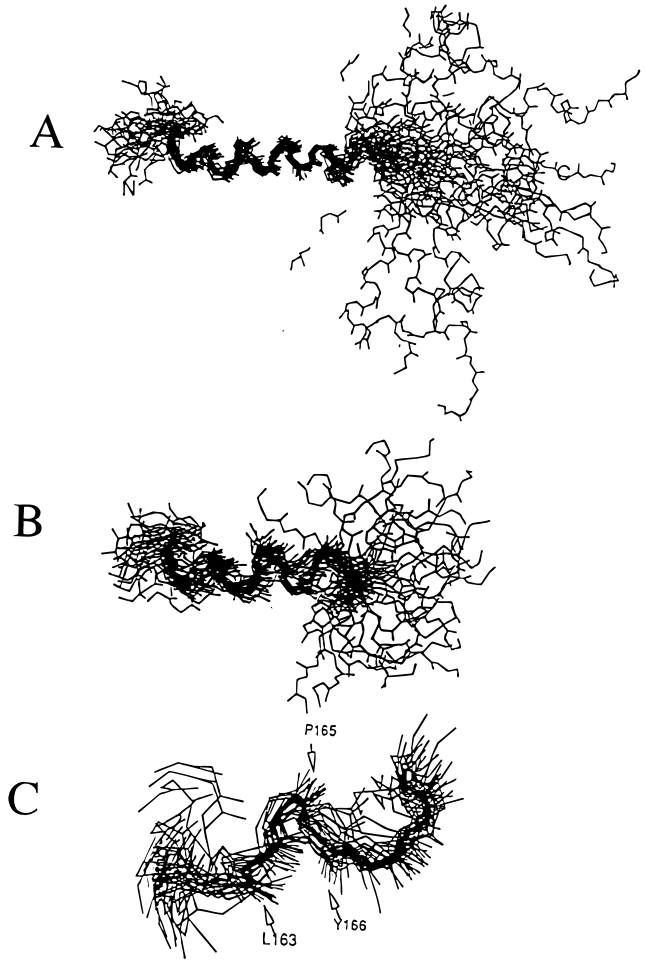

FIGURE 6: Backbone view of an ensemble of 29 structures out of 50 of apoA-I(142−187) in DPC at pH 4.9 and 37 °C (A) with residues 146−164 superimposed; (B) C-terminal helical structures with residues 170−181 superimposed; and (C) the interhelical structures, residues 161−169 with 163−168 superimposed.

apoA-I(142−187) in the presence of DPC using 450 NOEs (227 intra- and 223 interresidue). Superimposing the N-terminal helix (146−162) led to a "fraying" of the C-terminal helix (168−182) (Figure 6A) and vice versa, illustrating a hinge between the two helices, which correspond to helical repeats 5 and 6 in the intact protein. The RMSD for superimposing the backbone atoms of the helical region 146−162 is 0.98 ± 0.22 Å. Superimposing the backbone atoms of the helical region 168−182 (Figure 6B) gave a RMSD of 1.99 ± 0.42 Å. The better-defined N-terminal helix can be attributed to higher resolution (more NOE restraints resolved) of proton resonances. Finally, when 29 structures of the hinge region, residues 163−168, were superimposed (Figure 6C) they show that the hinge region resembles a helical-turn structure. The RMSD of the superimposed backbone atoms of the hinge region 163−168 is 1.11 ± 0.39 Å.

The structure of apoA-I(142−187) in SDS micelles was calculated based on 397 NOEs (195 inter- and 202 intraresidue). The RMSDs for superimposing the backbone atoms of the helical regions 146−162 (A) and 168−182 (B) are 2.38 ± 0.20 and 2.02 ± 0.21 Å, respectively. Superimposing the interhelical region gave a RMSD of 1.84 ± 0.20 Å. Therefore, the N-terminal helix residues 146−162 in SDS is not as well defined as in DPC. This may relate to the temperature at which the NOESY spectra were collected.

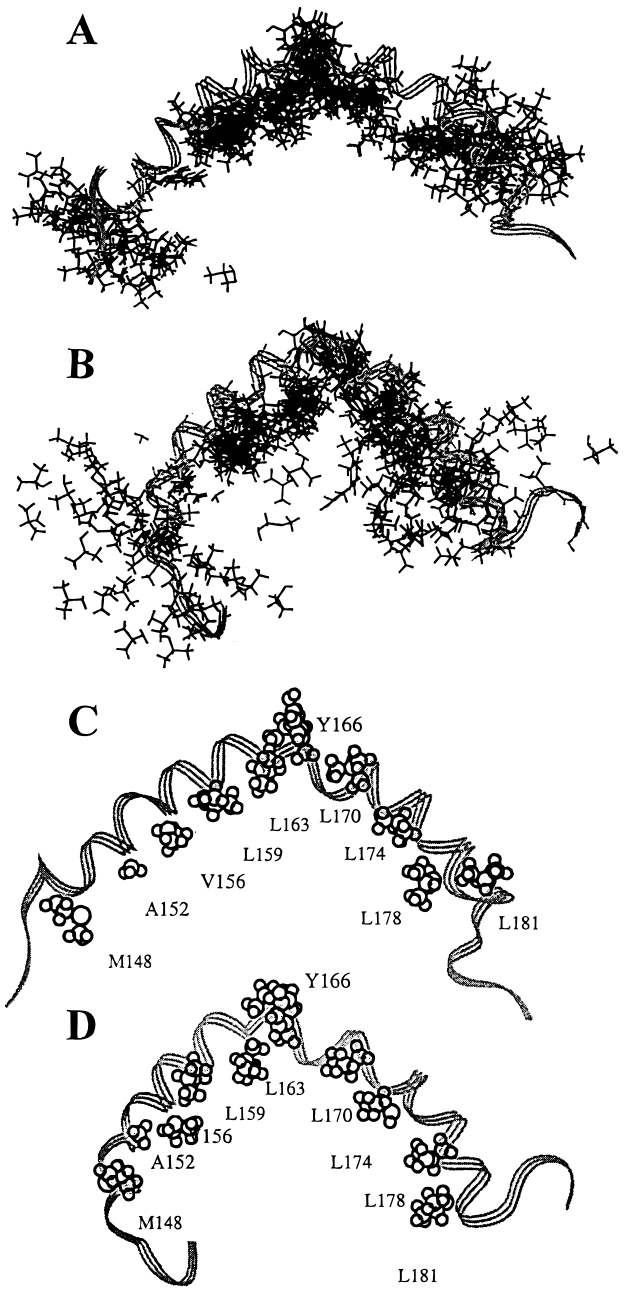

FIGURE 7: Ribbon representation of the structure most resembling the average of apoA-I(142−187) in DPC (panels A and C) or in SDS (panels B and D). In panels A and B, hydrophobic side chains of all the structures in the ensemble are given whereas in panels C and D only the hydrophobic side chains resembling the average ones are shown. The hydrophobic side chains show a high population on the concave face although it is more pronounced for those in the N-terminal helix than in the C-terminal helix, which is less well-defined. Note that Y166 stacks with P165 and interacts with SDS alkyl chain.

More NOEs were obtained in DPC at 37 °C (450 NOEs) than in SDS at 50 °C (397 NOEs). In both SDS and DPC micelles, the C-terminal helix is less well defined. This is best illustrated by Figure 7, panels A and B where the side chains of the C-terminal helix are more dispersed then those in the N-terminal helix. As well, the C-terminal residues 183−187 are unstructured due to lack of NOEs (Figure 5). Since two sets of TOCSY peaks were found for residues E183 and N184 there may be two highly populated conformers. In addition, zero-quantum peaks were found for G185 and G186 in the NOESY at a mixing time of 50 ms, suggesting that the region may be mobile (Cavanagh et al., 1996).

Figure 7 shows the average structures determined in DPC (A and C) and SDS (B and D). Both are curved helix-hinge-helix structures with the hydrophobic side chains on the concave face. It can also be seen that the aromatic ring of Y166 stacks with the ring of P165 with its hydroxyl group pointing toward the hydrophilic face. This local hydrophobic packing may explain why one of the H^{β} of P165 shifted upfield by approximately 1 ppm. Further investigation of the average structures showed that the dihedral angles (Φ and Ψ) for residues 146−162 and 168−182 fall within the helical region on the Ramachandran plot.

Intermolecular NOEs between ApoA-I(142−187) and SDS. NOESY spectra of apoA-I(142−187) (6 mM) were run in 50% SDS-d_{25}/50% SDS (total SDS = 60 mM) at pH 4.9 and 37 °C. Intermolecular NOEs with SDS alkyl chains were observed for the following residues: M148, H155, H162, Y166, K182, plus all the arginines. The NOE cross-peaks were observed at a mixing time of 40 ms and were clearer at 120 ms. The identification and assignment of these intermolecular NOE peaks were possible since the side chains of those residues have well-resolved proton resonances. The detection of intermolecular NOEs for Y166 and the arginines with SDS is consistent with our previous finding for apoA-I(166−185) (Wang et al., 1996b). These residues span the sequence from 148 to 182, indicating that both helices and the interhelical region bind SDS.

Peptide-Aided Signal Assignment of ApoA-I(122−187) and Intact ApoA-I. A portion of the NOESY spectrum of apoA-I(142−187) (46mer) in SDS is given in Figure 8A. The same spectral region of apoA-I(122−187) (66mer) in SDS is presented in Figure 8B. The spectral pattern observed for apoA-I(142−187) is evident in the same spectral region of apoA-I(122−187). Like patterns in the whole spectrum led to the complete assignment of the region 146−187 in the 66mer. In addition, the NOE connectivity pattern was similar for the region 146−187, indicating the helix-hinge-helix structural motif found in apoA-I(142−187) is retained in apoA-I(122−187). Figure 8C shows a portion of the NOESY spectrum of intact apoA-I in the presence of deuterated SDS. In the complete NOESY spectrum, only four Trp N1 proton signals were detected, suggesting that apoA-I in SDS is in the monomer state. The majority of H^{α} protons of apoA-I resonate to high field of the water signal, suggesting that the principal secondary structure in apoA-I is helical. Chemical shift assignments of the protons of R153, V156, A164, P165, and A175 were accomplished by comparison with similar spin patterns found in the two fragments (Figure 8, panels A and B). The assignment of these resonances could be attributed to their uniqueness in the apoA-I sequence and the unique NOE pattern found between A164 and P165. Finally, the ring current effect of Y166 in apoA-I shifted one H^{δ} of P165 upfield by ∼0.3 ppm relative to the random value listed by Wüthrich (1986), where fewer other resonances appear.

DISCUSSION

ApoA-I(166−185), apoA-I(142−187), and apoA-I(122−187) associate with SDS and DPC and adopt a helical conformation (Figure 1). It appears that a micelle is required for these peptides to bind DPC. Previously, apoA-I(148−

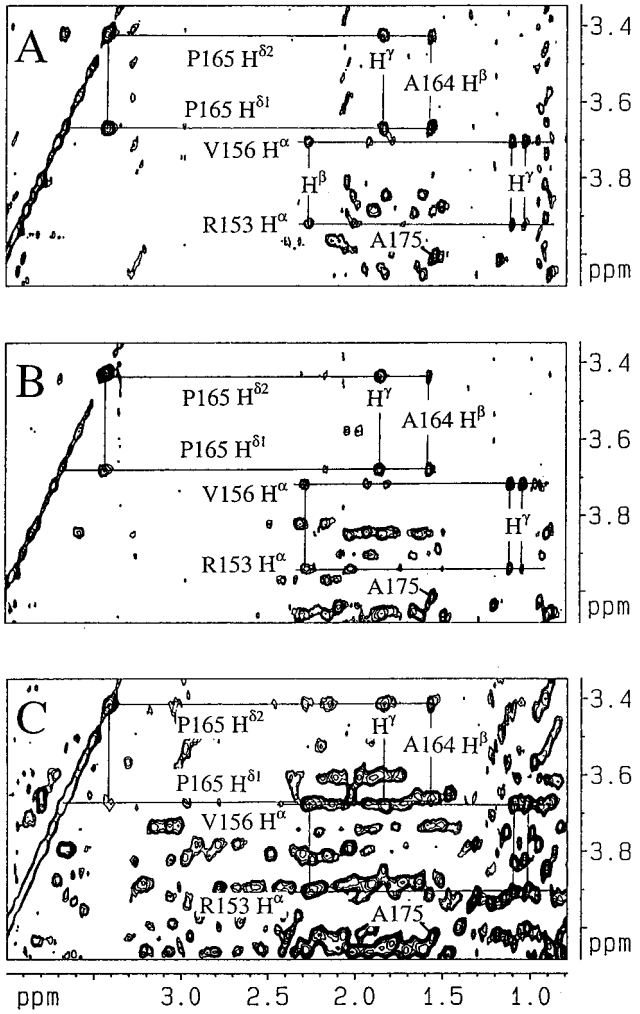

FIGURE 8: Portion of the NOESY spectrum of (A) apoA-I(142−187), peptide/SDS molar ratio 1:60, at pH 6.9 and 50 °C (τ_m = 150 ms), (B) apoA-I(122−187), peptide/SDS ratio 1:60, at pH 6.2 and 50 °C (τ_m = 300 ms), and (C) apoA-I, protein/SDS ratio 1:140, at pH 6.4 and 37 °C (τ_m = 150 ms). In each spectrum, only the NOE connetivities for P165 and A164, R153, and V156 were labeled.

185) (Sparrow & Gotto, 1980) and apoA-I(145−183) (Vanloo et al., 1995) were shown to bind to DMPC. In all these lipids, the predominant peptide conformation is helical (∼60−70%).

The NMR H^α secondary shifts of apoA-I(142−187) in either SDS or DPC micellar systems suggest two helical regions, residues 146−162 and 168−182, separated by a short proline-containing segment. The residues in the helical region correspond to ∼70% helix, similar to that found by CD. Superimposing the two helical regions leads to an ensemble of curved structures. The average angles between the two helices in the ensemble were estimated to be 130° in DPC and 90° in SDS. In the ensemble, there are 17% extended structures and 10% U-shaped (hairpin) with the remainder (73%) close to the average curved structures depicted in Figure 7. This, together with the observation of fewer, weaker NOEs in the region (Figure 5) and lack of long-range NOEs normally observed in globular proteins, suggests use of the term "hinge" (helix linker) to describe the interhelical structures of apoA-I(142−187) determined in micelles and to reflect the fact that the angle between the two helices is not well-defined. In both SDS and DPC, the peptide, on average, adopts curved amphipathic conformations with all the hydrophobic residues on the concave face (Figure 7).

The similarity in conformation of apoA-I(142−187), regardless of the lipid head group (Figure 7), reinforces our contention that the hydrophobic effect determines the overall conformation in the bound state (Buchko et al., 1996a,b; Wang et al., 1996a,b). However, electrostatic interactions also play a role, especially for class A amphipathic helices in the presence of anionic lipid. The interactions between positively charged peptide side chains and negatively charged SDS head groups may initiate binding (Figures 1 and 2), and once the helical structure is formed, they further stabilize the complexes. Existence of these electrostatic interactions between apoA-I peptides and SDS is supported by selective broadening of cationic and hydrophobic side-chain signals, the chemical shift differences of arginine side-chain ϵH^N resonances in SDS relative to DPC, the precipitation of these apoA-I peptides in SDS but not in DPC, and the higher thermal stability of apoA-I(142−187) complexed with SDS than with DPC (Figure 1D). Surewicz et al. (1986) found that apoA-I complexed with anionic lipids is much more stable than its complexes with zwitterionic lipids. Hence, our observations for apoA-I peptides in the two model lipids appear to be correlated with the data of others obtained for apoA-I.

In order to provide direct evidence for the peptide−lipid interactions, intermolecular NOESY experiments were performed in the presence of protonated SDS. Intermolecular NOE cross-peaks between SDS alkyl chains and the side chains of arginines, histidines, and the lysine confirmed that these side chains of the amphipathic helices are located in the interface of the peptide/SDS complexes and enhance the lipid affinity of class A1 amphipathic helices (Wang et al., 1996b). The NOEs of SDS with M148 and Y166 confirm the hydrophobic interactions. The involvement of Y166 in lipid binding is consistent with fluorescence spectroscopy (Figure 2). Hence, the two amphipathic helices, and the interhelical hinge, all associate with the hydrophobic core of the micelle. We propose a model for apoA-I(142−187)−lipid complexes, wherein the amphipathic helix-hinge-helix straddles the micelle.

In the proposed structures for the tandem helical repeats of apoA-I on discs, the protein is, almost without exception, depicted as a series of antiparallel amphipathic helices (the 11- and 22 mer repeats) linked by β-turns (Jonas et al., 1989; Brasseur et al., 1990). CD suggests that apoA-I conformation varies with the shape of the HDL particle (Sparks et al., 1992). Nevertheless, the parallel arrangement of helices is proposed to be maintained from discoidal to spherical particles (Brasseur et al., 1990; Sparks et al., 1992; Talussot & Ponsin, 1994). Since micelles with a diameter of ∼50−60 Å are comparable in size to the smallest HDL particles, they may be regarded as a good model for spherical HDL. In either SDS or DPC micelle models, no interhelix NOE was found in the spectrum of apoA-I(142−187), suggesting that helix 146−162 and helix 168−182 may not be closely packed. The helix−helix interactions, which have been proposed as an additional stabilizing force in apoA-I (Brasseur et al., 1990; Lins et al., 1995), do not occur in apoA-I(142−187) bound to micelles. This is consistent with the fact that both helices in apoA-I(142−187) are typical class A1 amphipathic helices (Segrest et al., 1994). A class A1

amphipathic helix contains positively charged amino acid residues located at the polar−nonpolar interface and negatively charged amino acid residues located at the center of the polar face. Thus, the helices of apoA-I(142−187), if tightly packed, would place repulsive cationic side chains in the interhelical region. In fact, all interfacial cationic side chains interact with lipid as shown in this study for apoA-I(142−187) and previously for apoA-I(166−185) (Wang et al., 1996b). Our straddle model may provide an alternative packing mode for helical repeats 5 and 6 in apoA-I in lipid.

The previous assignment of apoA-I(166−185) (Wang et al., 1996b) was found to be useful in assigning the spectra of apoA-I(142−187), and the conformation of residues 168−182 was subsequently found to be similar in the two peptides. The chemical shift similarity for residues 146−182 between apoA-I(142−187) and apoA-I(122−187) is more striking (Figure 8, panels A and B). By analogy, we were even able to assign several resonances in intact apoA-I (243 aa) (Figure 8C). We propose that such a peptide-aided signal assignment may be useful in NMR studies of apoA-I and other members in the exchangeable apolipoprotein family because of the periodicity in sequence. A similar strategy has recently been proposed for modular proteins (McEvoy et al., 1997).

Biological Implications. Our structural observations would indicate that the apoA-I structure in the middle part of the protein was designed by nature to be very flexible. Since the protein must serve several purposes depending on which lipoprotein particle it is located, it is understandable that the portion implicated in LCAT activation and cholesterol efflux should be readily accessible for interaction with the LCAT enzyme, CETP, or cellular receptors. Since these interactions are most likely different depending on the lipid composition and/or the size of the HDL particle, the protein must be able to change conformation to allow for these important biological functions. We believe that the helix-hinge-helix motif would permit the rapid change in structure needed to accommodate the multifunctional nature of apoA-I. Since the termini have been implicated in the rapid association of apoA-I with lipid, a flexible internal sequence would allow the protein to expose important functional regions or suppress them as the particle composition changes when cholesterol is converted to cholesteryl ester or is transferred. Indeed, von Eckardstein et al. (1993) noted that the P165R mutant of apoA-I is defective in promoting cholesterol efflux. Our structural model suggests that an arginine substitution would destroy the hydrophobic packing, e.g., between P165 and Y166, in the hinge structure (Figure 7). As a consequence, the helix-hinge-helix motif in apoA-I(142−187) may become a long helix due to the P165R mutation. If this is the case, the long helix, unable to conform to the curved HDL surface as well as the helix-hinge-helix motif does, might lead to an increased clearance of apoA-I and, thus, lower HDL-cholesterol levels as observed clinically (Epand et al., 1995). A similar conformational change in the hinge of the P143R mutant of apoA-I (Utermann et al., 1984) or P143E mutation in hedgehog apoA-I (Sparrow et al., 1995) may explain, at least in part, the lower LCAT activating ability of these mutants. Finally, not all putative helices in human apoA-I are punctuated by prolines. The C-terminus of apoA-I(142−187) is unstructured in either SDS or DPC micelles (Figures 5B and 6B), and such flexibility may not be due to purely end effects but may be due to G185 and G186. The flexibility in this region of apoA-I may explain why it is most susceptible to proteolysis (Ji & Jonas, 1995). As these glycines are highly conserved in the homologous sequences of apoA-I from other species, it seems that glycines signal an independent structural domain at the C-terminus of apoA-I, which is essential in rapid and strong lipid binding, but not in LCAT activation (Sparrow & Gotto, 1982; Ji & Jonas, 1995; Schmidt et al., 1995; Holvoet et al., 1996).

ACKNOWLEDGMENT

We are indebted to Dr. Jan Eva Doran (Swiss Red Cross, Switzerland) for the apoA-I sample. G.W. wishes to thank MacMillan−Bloedel as a recipient of the IMBB Graduate Scholarship during the research. We thank A. Rozek, R. Storjohann, and Drs. R. B. Cornell (Simon Fraser University), R. O. Ryan, and V. Narayanaswami (University of Alberta) for useful discussions.

SUPPORTING INFORMATION AVAILABLE

Tables showing proton chemical shifts (in parts per million) of apoA-I(142−187) in H_2O/D_2O, 9:1 (v/v), pH 4.9, 37 °C (50 °C), in DPC-d_{38} (SDS-d_{25}) micelles, peptide/DPC-(SDS) molar ratio of 1:60 (6 pages). Ordering information is given on any current masthead page.

REFERENCES

Acton, S., Rigotti, A., Landschulz, K. T., Xu, S., Hobbs, H. H., & Krieger, M. (1996) *Science 271*, 518−520.

Anantharamaiah, G. M., Venkatachalapathi, Y. V., Brouillette, C. G., & Segrest, J. P. (1990) *Arteriosclerosis 10*, 95−105.

Banka, C. L., Bonnet, D. J., Black, A. S., Smith, R. S., & Curtiss, L. K. (1991) *J. Biol. Chem. 266*, 23886−23892.

Barany, G., & Merrifield, R. B. (1980) in *The Peptides: Analysis, Synthesis, Biology* (Gross, E., & Meienhofer, J., Eds.) pp 3−284, Academic Press, New York.

Bax, A., & Davis, D. G. (1985) *J. Magn. Reson. 65*, 355−360.

Brasseur, R., De Meutter, J., Vanloo, B., Goormaghtigh, E., Ruysschaert, J. M., & Rossenneu, M. (1990) *Biochim. Biophys. Acta 1043*, 245−252.

Braunschweiler, L., & Ernst, R. R. (1983) *J. Magn. Reson. 53*, 521−528.

Breslow, J. L. (1996) *Science 272*, 685−688.

Brewer, H. B.,Jr., Fairwell, T., LaRue, A., Ronan, R., Houser, A., & Bronzert, T. J. (1978) *Biochem. Biophys. Res. Commun. 80*, 623−630.

Buchko, G. W., Treleaven, W. D., Dunne, S. J., Tracey, A. S., & Cushley, R. J. (1996a) *J. Biol. Chem. 271*, 3039−3045.

Buchko, G. W., Wang, G., Pierens, G. K., & Cushley, R. J. (1996b) *Int. J. Pept. Protein Res. 48*, 21−30.

Castro, G. R., & Fielding, C. J. (1988) *Biochemistry 27*, 25−29.

Cavanagh, J., Fairbrother, W. J., Palmer, A. G., III, & Skelton, N. J. (1996) *Protein NMR Spectroscopy, Principles and Practice*, Academic Press, New York.

Clore, G., Gronenborn, A., Nilges, M., & Ryan, C. (1987) *Biochemistry 26*, 8012−8023.

Englander, S. W., & Wand, A. J. (1987) *Biochemistry 26*, 5953−5958.

Epand, R. M., Shai, Y., Segrest, J. P., & Anantharamaiah, G. M. (1995) *Biopolymers 37*, 319−338.

Fielding, C. J., Shore, V. G., & Fielding, P. E. (1972) *Biochem. Biophys. Res. Commun. 46*, 1493−1498.

Fielding, P. E., Kawano, M., Catapano, A. L., Zoppo, A., Marcovina, S., & Fielding, C. J. (1994) *Biochemistry 33*, 6981−6985.

Freifelder, D. (1976) *Physical Biochemistry. Application to Biochemistry and Molecular Biology*, pp 410−443, W. H. Freeman and Company, San Francisco.

Fukushima, D., Yokoyama, S., Kroon, D. J., Kezdy, F. J., & Kaiser, E. T. (1980) *J. Biol. Chem. 255*, 10651−10657.

Gill, S. C., & von Hippel, P. H. (1989) *Anal. Biochem. 182*, 319−326.
Glomset, J. A. (1968) *J. Lipid Res. 9*, 155−167.
Gronenborn, A. M., & Clore, G. M. (1995) *CRC Crit. Rev. Biochem. Mol. Biol. 30*, 351−385.
Hancock, W. S., & Sparrow, J. T. (1981) *J. Chromatogr. 206*, 71−82.
Hancock, W. S., & Sparrow, J. T. (1984) *Chromatographic Science Series*, Vol. 26, Marcel Dekker, Inc., New York.
Havel, T. F. (1991) *Prog. Biophys. Mol. Biol. 56*, 43−78.
Helenius, A., & Simons, K. (1975) *Biochim. Biophys. Acta 415*, 29−79.
Henry, G. D., & Sykes, B. D. (1994) *Methods Enzymol. 239*, 515−535.
Holvoet, P., Zhao, Z., Vanloo, B., Vos, R., Deridder, E., Dhoest, A., Taverrne, J., Brouwers, E., Demarsin, E., Engelborghs, Y., Rosseneu, M., Collen, D., & Brasseur, R. (1995) *Biochemistry 34*, 13334−13342.
Holvoet, P., Zhao, Z., Deridder, E., Dhoest, A., & Collen, D. (1996) *J. Biol. Chem. 271*, 19395−19401.
Holzwarth, G., & Doty, P. (1965) *J. Am. Chem. Soc. 87*, 218−228.
Jeener, J., Meier, B. H., Bachmann, P., & Ernst, R. R. (1979) *J. Chem. Phys. 71*, 4546−4553.
Ji, Y., & Jonas, A. (1995) *J. Biol. Chem. 270*, 11290−11297.
Jonas, A., Kézdy, K. E., & Wald, J. H. (1989) *J. Biol. Chem. 264*, 4818−4824.
Lauterwein, J., Bösch, C., Brown, L. R., & Wüthrich, K. (1979) *Biochim. Biophys. Acta 556*, 244−264.
Lins, L., Brasseur, R., De Pauw, M., Van Biervliet, J. P., Ruysschaert, J.-M., Rosseneu, M., & Vanloo, B. (1995) *Biochim. Biophys. Acta 1258*, 10−18.
Marion, D., & Wüthrich, K. (1983) *Biochem. Biophys. Res. Commun. 113*, 967−974.
Marion, D., Ikura, M., & Bax, A. (1989) *J. Magn. Reson. 84*, 425−430.
McDonnell, P. A., & Oppella, S. J. (1993) *J. Magn. Reson. B102*, 102−125.
McEvoy, M. M., de la Cruz, A. F. A., & Dahlquist, F. W. (1997) *Nat. Struct. Biol. 4*, 9.
McLachlan, A. D. (1977) *Nature (London) 267*, 465−466.
Meng, Q.-H., Calabresi, L., Fruchart, J.-C., & Marcel, Y. L. (1993) *J. Biol. Chem. 268*, 16966−16973.
Minnich, A., Collet, X., Roghani, A., Cladaras, C., Hamilton, R. L., Feilding, C. J., & Zannis, V. I. (1992) *J. Biol. Chem. 267*, 16553−16560.
Mysels, K. J., & Pricen, L. H. J. (1959) *J. Phys. Chem. 63*, 1696−1700.
Nakagawa, S. H., Lau, H. S. H., Kézdy, F. J., & Kaiser, E. T. (1985) *J. Am. Chem. Soc. 107*, 7087−7092.
Narayanaswami, V., Kay, C. M., Oikawa, K., & Ryan, R. O. (1994) *Biochemistry 33*, 13312−13320.
O'Neil, J. D. J., & Sykes, B. D. (1989) *Biochemistry 28*, 699−707.
Perczel, A., Hollósi, M., Tusnády, G., & Fasman, G. D. (1991) *Protein Eng. 4*, 669−679.
Piotto, M., Saudek, V., & Sklenár, V.(1992) *J. Biomol. NMR 2*, 661−665.
Rance, M., Sørensen, O. W., Bodenhausen, G., Wagner, G. Enrst, R. R., & Wüthrich, K. (1983*) Biochem. Biophys. Res. Commun. 117*, 479−485.
Redfield, A. G., & Kuntz, S. D. (1975) *J. Magn. Reson. 19*, 250−254.
Reid, G. E., & Simpson, R. J. (1992) *Anal. Biochem. 200*, 301−309.
Reynolds, J. A. (1982) in *Lipid-Protein Interactions* (Jost, P. C., & Griffith, O. H., Eds.) Vol. 2, pp 193−224, Wiley, New York.
Rogers, D. P., Brouillette, C. G., Engler, J. A., Tendian, S. W., Roberts, L., Mishra, V. K., Anantharamaiah, G. M., Lund-Katz, S., Phillips, M. C., & Ray, M. J. (1997) *Biochemistry 36*, 288−300.
Rozek, A., Buchko, G. W., & Cushley, R. J. (1995) *Biochemistry 34*, 7401−7408.
Scanu, A. M., Edelstein, C., & Shen, B. W. (1982) in *Lipid-Protein Interactions* (Jost, P. C., & Griffith, O. H., Eds.) Vol. 1, pp 259−316, John Wiley and Sons, New York.
Schmidt, H. H.-J., Remaley, A. T., Stonik, J. A., Ronan, R., Wellmann, A., Thomas, F., Zech, L. A., Brewer, H. B., Jr., & Hoeg, J. M. (1995) *J. Biol. Chem. 270*, 5469−5475.
Segrest, J. P., Jackson, R. L., Morrisett, J. D., & Gotto, A. M. (1974) *FEBS lett. 38*, 247−253.
Segrest, J. P., Garber, D. W., Brouillette, C. G., Harvey, S. C., & Anantharamaiah, G. M. (1994) *Adv. Protein Chem. 45*, 303−369.
Sklenár, V., Piotto, M., Leppik, R., & Saudek, V. (1993) *J. Magn. Reson. A102*, 241−245.
Sorci-Thomas, M. G., Kearns, M. W., & Lee, J. P. (1993) *J. Biol. Chem. 268*, 21403−21409.
Sorci-Thomas, M. G., Curtiss, L., Parks, J. P., Thomas, M. J., & Kearns, M. W. (1997) *J. Biol. Chem. 272*, 7278−7284.
Sparks, D. L., Lund-katz, S., & Phillips, M. C. (1992) *J. Biol. Chem. 267*, 25839−25847.
Sparrow, D. A., Laplaud, P. M., Saboureau, M., Zhou, G., Dolphin, P. J., Gotto, A. M., Jr., & Sparrow, J. T. (1995) *J. Lipid Res. 36*, 485−495.
Sparrow, J. T. (1976) *J. Org. Chem. 41*, 350−1353.
Sparrow, J. T., & Gotto, A. M. (1980) *Ann. NY Acad. Sci. 348*, 187−211.
Sparrow, J. T., & Gotto, A. M. (1982) *CRC Crit. Rev. Biochem. 13*, 87−107.
Sparrow, J. T., & Monera, O. D. (1996) *Pept. Res. 9*, 218−222.
Surewicz, W. K., Epand, R. M., Pownell, H. J., & Hui, S.-W. (1986) *J. Biol. Chem. 261*, 16191−16197.
Sviridov, D., Pyle, L., & Fidge, N. (1996) *Biochemistry 35*, 189−196.
Talussot, C., & Ponsin, G. (1994) *J. Theor. Biol. 169*, 143−152.
Uboldi, P., Spoladore, M., Fantappiè, S., Marcovina, S., & Catapano, A. L. (1996) *J. Lipid Res. 37*, 2557−2568.
Utermann, G., Haas, J., Steinmetz, A., Pattzold, R., Rall, S. C., Weisgraber, K. H., & Mahley, R. W. (1984) *Eur. J. Biochem. 144*, 326−331.
Vanloo, B., Demoor, L., Boutillon, C., Lins, L., Brasseur, R., Baert, J., Fruchart, J. C., Tartar, A., & Rosseneu, M. (1995) *J. Lipid Res. 36*, 1686−1696.
von Eckardstein, A., Castro, G., Wybranska, I., Theret, N., Duchateau, P., Duverger, N., Fruchart, J. C., Ailhaud, G., & Assman, G. (1993) *J. Biol. Chem. 268*, 2616−2622.
Wang, G., Pierens, G. K., Treleaven, W. D., Sparrow, J. T., & Cushley, R. J. (1996a) *Biochemistry 35*, 10358−10366.
Wang, G., Treleaven, W. D., & Cushley, R. J. (1996b) *Biochim. Biophys. Acta 1301*, 174−184.
Wishart, D. S., Sykes, B. D., & Richards, F. M. (1992) *Biochemistry 31*, 1647−1651.
Woody, R. W. (1995) *Methods Enzymol. 246*, 34−71.
Wüthrich, K. (1986) *NMR of Proteins and Nucleic Acids*, Wiley, New York.
Wüthrich, K., Billeter, M., & Braun, W. (1983) *J. Mol. Biol. 169*, 949−961.
Wüthrich, K., Billeter, M., & Braun, W. (1984) *J. Mol. Biol. 180*, 715−740.
Zhao, Y., Sparks, D. L., & Marcel, Y. L. (1996) *J. Biol. Chem. 271*, 25145−25151.

BI971151Q